Detection of defects in photovoltaic modules through electroluminescence image analysis

Amanda A. Alvim[1], Gilberto Figueiredo[1], André da Costa Pinho[1]

[1] Fluminense Federal University, Niterói (Brazil)

Abstract

This work explores the use of machine learning techniques to automate defect detection in photovoltaic (PV) modules through electroluminescence (EL) image analysis. Four approaches were examined: Convolutional Neural Networks (CNNs), Wavelet Scattering with traditional classifiers, Wavelet Scattering combined with CNNs, and a modified VGG16 architecture. Experimental results, based on a dataset of 2,435 EL images from mono- and polycrystalline silicon PV cells, showed high classification accuracy—especially when preprocessing techniques were applied. These findings support the integration of EL imaging and machine learning for fault diagnosis in PV systems.

Keywords: Electroluminescence, solar cell defects, machine learning, wavelet scattering.

1. Introduction

The growth of solar energy in the global energy scenario highlights the need for strict quality control of photovoltaic (PV) cells and modules along production lines. Such control ensures the long-term reliability of PV systems and minimizes the risks of premature failures. In large-scale PV plants, quality assurance is a decisive factor for both technical and economic viability, as performance indices directly affect financial returns (I. De La Parra et al., 2017). To guarantee product reliability, non-destructive testing methods are widely used, including electrical characterization such as current–voltage (I–V) curve analysis, performed under different operating conditions. Qualification procedures standardized by IEC 61215 also cover mechanical and environmental evaluations to verify compliance with international standards (A. Alvim and G. Figueiredo, 2023).

Among complementary techniques, such as Laser Beam Induced Current (LBIC) spectroscopy and Electron Beam Induced Current (EBIC), electroluminescence (EL) imaging has emerged as a powerful and practical diagnostic tool for revealing defects invisible to the naked eye. By forward-biasing a PV cell or module, EL captures near-infrared emissions that expose structural irregularities such as microcracks, busbar interruptions, and soldering failures - issues that may not be evident in conventional I–V analyses. Owing to its sensitivity and simplicity, EL imaging has become an essential complement to traditional electrical testing in ensuring the quality and durability of PV modules (T. Mchedlidze et al., 2016; R. Ebner et al., 2013).

However, EL image evaluation is often performed manually, which is time-consuming and dependent on expert interpretation. In large-scale installations with thousands of modules, manual assessments become impractical and can delay maintenance actions. This study addresses the growing need for efficient and reliable methods to detect PV module defects through automated analysis. By applying machine learning algorithms to EL images, the proposed approach aims to recognize defects accurately and consistently, supporting large-scale inspection and maintenance of PV plants.

2. Electroluminescence Imaging in Photovoltaic Modules

2.1. Electroluminescent Emission in PV Cells

Electroluminescence (EL) is the reverse process of photovoltaic energy conversion. Instead of converting light into electricity, electrical energy is transformed into electromagnetic radiation within the near-infrared range (900–1300 nm), which is invisible to the human eye. This emission occurs when electrons are injected into a semiconductor and recombine radiatively across the silicon energy bands. The intensity of the emitted radiation depends on the concentration of minority carriers and on the efficiency of the pn junction in separating electrons and holes, which in turn affects the open-circuit voltage of the cell (T. Fuyuki et al., 2007).

10.18086/swc.2025.03.18 Available at http://proceedings.ises.org

In practice, EL imaging requires forward biasing a PV cell or module using a direct-current source capable of controlling both voltage and current. Images are typically captured under two bias conditions: at the short-circuit current (Isc) and at 10% of Isc, as showed in figures 1 and 2 respectively. While full Isc illumination provides enough brightness to reveal general defect patterns, the lower current level is especially useful for identifying cells affected by potential-induced degradation (PID). Under these conditions, variations in brightness and contrast reveal both structural and electrical nonuniformities across the module surface (T. Fuyuki et al., 2005; M. Köntges et al., 2009).

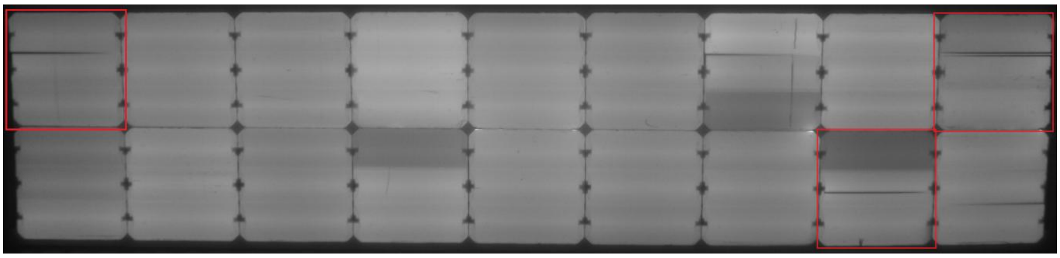

Figure 1: Image captured applying the short-circuit current.

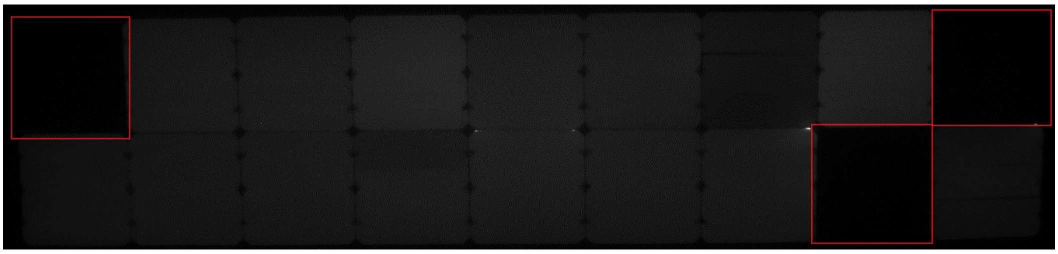

Figure 2: Image captured applying 10% of the short-circuit current.

2.2. Electroluminescence imaging

Since the emitted radiation lies in the infrared spectrum, specialized sensors are required to acquire EL images. Cameras equipped with indium gallium arsenide (InGaAs) or germanium (Ge) detectors are most commonly used owing to their high sensitivity and fast response in the near-infrared region. These devices allow the visualization of microcracks, shunts, and other structural anomalies that are otherwise invisible to the naked eye.

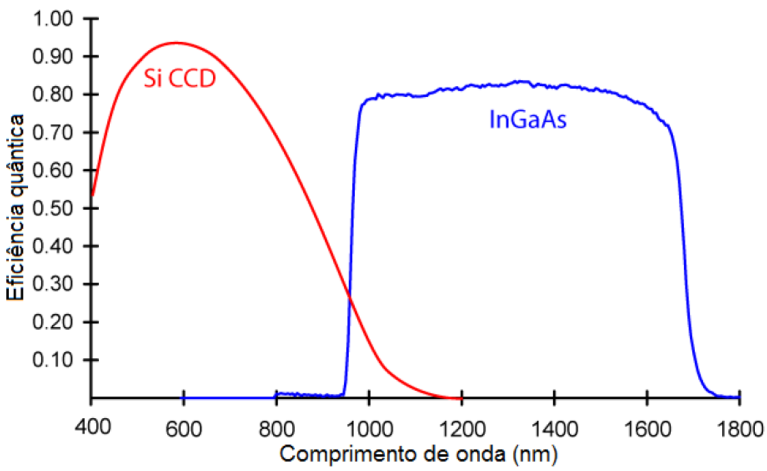

Figure 3: Spectral sensitivity of silicon and InGaAs-based CCD sensors (G. Figueiredo et al.et al., 2018).

Conventional charge-coupled device (CCD) cameras based on silicon sensors can also be employed as a low-cost alternative. Although their quantum efficiency within the EL emission band is lower than that of InGaAs sensors, as illustrated in Figure 3, CCDs can still produce satisfactory images when acquisition conditions are optimized—preferably in dark environments to minimize ambient light interference. This makes CCD cameras an accessible option for laboratory or controlled-environment inspections (G. Figueiredo et al.et al., 2018). For field applications where ambient illumination is unavoidable, additional adaptations may be necessary. A practical low-cost solution is to couple a near-infrared (NIR) optical filter to the imaging system, which allows EL acquisition without requiring complete darkness.

2.3. Defects in PV Modules Detected by EL Imaging

Photovoltaic modules are susceptible to a variety of defects that may arise during manufacturing, transportation, installation, or long-term exposure to environmental stresses such as wind loads, snow accumulation, and humidity. These defects can significantly reduce module performance and reliability over time. To address these challenges, the IEC TS 60904-13 standard provides recommendations for interpreting the different types of detectable defects. Early identification of such failures is crucial to maintaining the efficiency and durability of PV installations.

Appendix C of this specification defines a diagnostic procedure for quantifying cell cracks—one of the most common and detrimental defect types. Cracks are classified into three modes according to their electrical severity. Mode A corresponds to discrete microcracks that do not compromise the active cell area. Mode B includes cracks that partially disconnect electrically active regions, producing medium-contrast zones in EL images captured at Isc. Mode C describes severe cracks that isolate significant portions of the cell, resulting in high-contrast regions in both full and reduced bias images. Mode C defects cause major performance losses and may induce local reverse-bias conditions, leading to **hot spots**—localized overheating that accelerates degradation and, in severe cases, results in permanent module failure. Figure 4 illustrates these crack modes and their increasing impact on electrical performance.

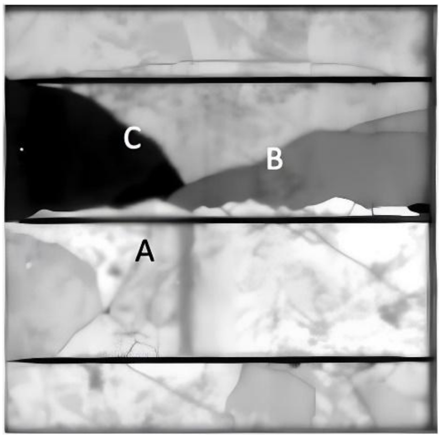

Figure 4: Crack modes (IEC TS 60904-13, 2018)

Beyond cracking, EL imaging can reveal several other defect categories commonly observed in crystalline-silicon modules. These include missing or broken grid fingers, delamination, and contamination from manufacturing residues—all of which create localized shunts and reduce carrier lifetime. Potential-induced degradation (PID) typically appears as widespread cell darkening under reduced bias. Ribbon bonding failures and poor soldering manifest as regions of elevated series resistance, often precursors to hot-spot formation. Other detectable issues include wafer impurities, solder-flux residues interacting with metallization, and surface discolorations caused by processing inconsistencies.

2.4 Image Processing for EL Analysis

For machine learning models to operate effectively, EL images must first undergo preprocessing to correct acquisition-related imperfections such as noise, diffuse illumination, and geometric distortions. Even under controlled conditions, achieving uniform focus, exposure, and alignment is challenging, and such inconsistencies can hinder large-scale analysis. Automated preprocessing is therefore essential to standardize image properties—resolution, brightness, and perspective—across datasets used for training and validation.

The IEC TS 60904-13 standard recommends mitigating diffuse illumination by subtracting frames of energized and non-energized modules. Vignetting effects, where darker edges obscure defect regions, can be corrected by capturing a reference image to estimate the vignette extent and applying a normalization matrix to adjust pixel intensities.

Several tools support these preprocessing procedures. Proprietary environments such as MATLAB provide advanced image-processing functions, while open-source libraries like Python Imaging Library (PIL), OpenCV, and Scikit-image offer flexible, high-performance alternatives. These can be integrated with NumPy for efficient pixel-matrix manipulation. Regardless of the software used, preprocessing remains an indispensable step to ensure homogeneity and reliability in EL datasets.

3. Machine Learning for Defect Detection in PV Modules

3.1. Overview of Machine Learning Techniques

Machine learning (ML) is a subfield of artificial intelligence that enables systems to learn from data, identify patterns, and make decisions with minimal human intervention. In the context of photovoltaic (PV) systems, ML has been increasingly applied to defect detection in electroluminescence (EL) images, as demonstrated by several recent studies (W. Tang et al.et al., 2020; M. Dhimish, 2021; M. Y. Demirci, 2021; Y. Wang, 2021). Most approaches frame the problem as binary classification, distinguishing between defective and non-defective cells.

ML techniques can be categorized into four main learning paradigms: supervised, unsupervised, semi-supervised, and reinforcement learning. In supervised learning, algorithms are trained using labeled datasets, learning the mapping between input features—such as pixel intensities or extracted image descriptors—and their corresponding output classes. This approach is particularly effective for tasks such as regression and classification and is widely used in PV defect detection (U. Jahn et al., 2018; A. Mellit and S. Kalogirou, 2021).

In contrast, unsupervised learning deals with unlabeled data, identifying hidden structures or relationships among samples. It is useful for clustering or anomaly detection, especially when labeled data are scarce. Reinforcement learning employs a reward-based mechanism, where an agent interacts with an environment and learns optimal actions through feedback. Finally, semi-supervised learning combines both labeled and unlabeled data, leveraging the structure of the data to improve learning performance when labeling is costly or time-consuming. Each paradigm offers unique advantages depending on dataset availability and the level of supervision feasible for the inspection process.

3.2. Convolutional Neural Networks (CNNs)

Convolutional Neural Networks (CNNs) are a class of deep learning models inspired by the visual cortex of the human brain, specifically designed to recognize patterns and extract relevant features from large volumes of visual data. Unlike traditional machine learning methods such as Support Vector Machines (SVM), CNNs learn hierarchical representations of data, making them particularly effective in analyzing complex image patterns.

CNN architectures consist of multiple layers, each performing specific functions. Convolutional layers apply filters (kernels) to the input image, generating feature maps that highlight local structures such as edges, textures, or shapes, while preserving spatial relationships between pixels. Pooling layers then reduce the dimensionality of these maps by summarizing information within smaller regions, which helps decrease computational complexity and increase model robustness. The output is later flattened into a one-dimensional vector and passed to fully connected layers, which combine the extracted features to perform classification or regression tasks through activation functions.

Although CNNs have proven to be highly effective in a wide range of computer vision applications—such as image classification, object detection, and facial recognition—their training demands substantial computational resources. Graphics Processing Units (GPUs) play a critical role in this context, as their parallel processing architecture significantly accelerates the large-scale matrix operations required in deep learning (M. W. Akram *et al.*, 2018). Despite the high computational cost, CNNs remain the state-of-the-art approach for automated image analysis, including defect detection in PV modules.

3.3. Wavelet Scattering Transform (WST)

Wavelet scattering is a feature extraction technique designed for efficient analysis of data such as time series and images. Its primary goal is to capture meaningful representations that can be used as input for machine learning algorithms. A key advantage of this method is its stability to small transformations: it is largely unaffected by shifts, rotations, or deformations of the input, which is particularly useful when analyzing images where objects may appear displaced or rotated.

The method works by decomposing data into multiple scales using mathematically predefined filters called wavelets. This multiscale representation captures both coarse and fine patterns, providing a comprehensive description of the signal or image. Unlike CNNs, which require filters to be learned during training, wavelet scattering uses fixed filters, reducing the complexity of the learning process.

This property makes WST especially valuable in scenarios with limited data availability, as it avoids the overfitting risks associated with high-capacity deep networks. The resulting scattering coefficients can then be fed into classical classifiers, such as Support Vector Machines (SVM) or k-Nearest Neighbors (kNN), to perform the final classification task. This approach offers high robustness and reduced computational cost, which is advantageous for embedded PV inspection systems where resources are limited.

4. Methodology and Experimental Setup

The methodology adopted in this work was structured to enable the development, training, and evaluation of machine learning (ML) models for automated defect detection in photovoltaic (PV) modules using electroluminescence (EL) images. The process was divided into four main stages: dataset preparation, image preprocessing, models implementation, and performance evaluation. The overall workflow is summarized in Figure 5.

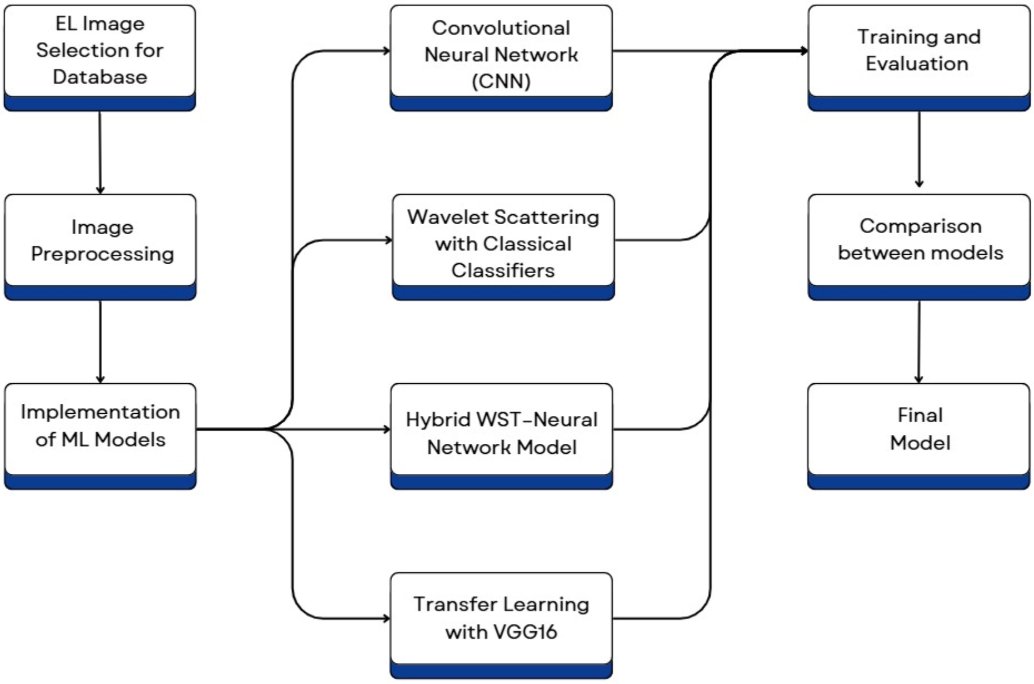

Figure 5: Methodology flowchart.

4.1. Dataset Preparation

The EL images used in this study were obtained from publicly available databases introduced by Buerhop-Lutz et al. (C. Buerhop-Lutz et al., 2018; S. Deitsch et al., 2019, 2021), which contains EL images of PV cells extracted from monocrystalline and polycrystalline modules. After an initial review and curation process to remove low-quality or duplicated images, two datasets were organized to support different training scenarios.

The reduced dataset contained 600 images, equally divided between monocrystalline and polycrystalline cells (300 each), with balanced representation of the defective and non-defective classes. The expanded dataset comprised 2,435 images (1,065 monocrystalline and 1,370 polycrystalline), also balanced between the two classes.

These two subsets were employed to test different training strategies, involving both original and pre-processed images. For each subset, six training configurations were considered: models trained exclusively with monocrystalline cells, exclusively with polycrystalline cells, and with a combination of both, each case being repeated with either raw or pre-processed images. This design allowed for a systematic assessment of the influence of cell type and preprocessing on model performance.

In total, 24 simulations were conducted with the reduced dataset (six configurations applied to four different models). The same procedure was repeated with the extended dataset, producing another 24 training runs, this time using all 2,435 available images.

4.2. Image Preprocessing

Before training, all EL images underwent preprocessing to improve uniformity and reduce acquisition artifacts. The steps included resizing, grayscale normalization, contrast enhancement, and augmentation through rotations and reflections to expand the dataset and mitigate overfitting.

Preprocessing was implemented using Python with OpenCV and NumPy libraries, following the guidelines of IEC TS 60904-13. A Contrast Limited Adaptive Histogram Equalization (CLAHE) was applied to improve local contrast and highlight fine defect patterns. The process began with the computation of average brightness and contrast values for each image, using statistical measures of pixel intensity distribution. These metrics served as indicators of visual quality and guided the subsequent corrections. After this evaluation, normalization was performed by scaling pixel values from the range [0, 255] to [0, 1].

For experiments labeled as preprocessed, these enhanced images were used directly in model training. For original configurations, raw EL images were used without corrections. This dual approach enabled quantitative assessment of how preprocessing influenced classification performance.

4.3 Implementation of Machine Learning Models

Four machine learning models were implemented to evaluate different strategies for detecting defects in electroluminescence (EL) images of photovoltaic (PV) modules: a Convolutional Neural Network (CNN), a Wavelet Scattering Transform (WST) with classical classifiers, a Hybrid WST–Neural Network model, and a Transfer Learning approach based on VGG16. All models were implemented in Python, using the TensorFlow and Keras frameworks for deep learning and kymatio for scattering.

4.3.1 Convolutional Neural Network (CNN)

The first approach implemented a custom CNN architecture inspired by classical deep learning models for image recognition. The network comprised three convolutional layers with increasing filter depth (32, 64, and 128), followed by max-pooling and batch normalization. ReLU activation was used in hidden layers and sigmoid in the output for binary classification.

The model was trained using the Adam optimizer, which automatically adjusts the learning rate for each parameter, accelerating convergence and reducing manual tuning, batch size of 32 and 120 epochs. This architecture was chosen for its strong ability to learn spatial hierarchies of features directly from pixel intensities, enabling robust discrimination between defective and non-defective cells.

4.3.2 Wavelet Scattering with Classical Classifiers

In the second approach, the Wavelet Scattering Transform (WST) was employed as a fixed feature extractor, followed by traditional machine learning classifiers. The WST provides a mathematically stable representation of image features by applying predefined wavelet filters at multiple scales and orientations, eliminating the need for learned kernels.

The resulting scattering coefficients were used to train classifiers such as Support Vector Machine (SVM), k-Nearest Neighbors (kNN), Random Forest, and others. Final decisions were obtained through majority voting among all classifiers, enhancing robustness and reducing model bias. This combination leveraged the descriptive power of WST while retaining the simplicity and interpretability of classical classifiers. It was particularly advantageous for smaller datasets, where overfitting in deep networks tends to occur.

4.3.3 Hybrid WST–Neural Network Model

To combine the advantages of handcrafted and learned representations, a hybrid model was developed in which WST features served as input to a shallow feedforward neural network. The network included a flatten layer followed by a dense output layer with sigmoid activation for binary classification, trained using the Adam optimizer and binary cross-entropy loss.

The logic behind this design was to leverage the advantages of both methodologies. On one hand, WST eliminates the need for learning convolutional filters from scratch, thus reducing computational cost and improving robustness when training data are limited. On the other hand, neural networks provide greater flexibility and non-linear modeling capacity than classical algorithms, enabling the extraction of higher-level interactions among scattering coefficients.

This hybrid architecture bridged the gap between classical methods and deep learning approaches. By integrating fixed mathematical representations with a trainable neural architecture, the model was expected to achieve a balance between efficiency and adaptability, offering a potentially more scalable framework for EL image classification.

4.3.4 Transfer Learning with VGG16

The final approach used transfer learning with the VGG16 architecture pre-trained on ImageNet. Since the original model was designed for RGB input, grayscale EL images were expanded to three channels using array replication and normalized to the [0, 1] range. Standard data augmentation techniques were also applied to increase the variability and robustness of the training dataset.

The convolutional base of VGG16 was frozen as a fixed feature extractor, while a new classification head was added, consisting of a flatten layer, a fully connected layer, dropout regularization and a sigmoid output neuron for binary classification. This transfer learning approach used the rich feature representations learned from ImageNet while adapting the network to the specific visual characteristics of electroluminescence images.

4.4 Training and Validation Procedure

Model evaluation was conducted using well-established classification metrics, including accuracy, precision, recall, F1-score, and the confusion matrix, providing a comprehensive assessment of model performance. All metrics were calculated on the test set, corresponding to 20% of the total dataset, which remained unseen during training to ensure unbiased evaluation.

Accuracy was adopted as the main indicator, representing the overall proportion of correctly classified samples. However, since accuracy alone may be misleading in imbalanced datasets, precision and recall were also analyzed to better capture each model's sensitivity and specificity. The F1-score, which combines precision and recall, provided a balanced view of the model's ability to correctly identify defective and non-defective cells. In addition, confusion matrices were examined to visualize classification errors, allowing for a detailed understanding of false positives and false negatives.

Finally, macro-average and weighted-average metrics were used to summarize model behavior across classes. The macro-average gives equal importance to each class, while the weighted-average accounts for differences in class size. Together, these indicators ensured a reliable and consistent evaluation of model performance across all tested configurations.

5. Results and Discussion

Results consistently improved when images were preprocessed, which reduced intra-class variability and markedly enhanced generalization on the larger dataset. Training on the expanded set (2,435 images) with preprocessing produced the best and most stable results, while models trained on the reduced set tended to show artificially higher scores due to overfitting.

The Convolutional Neural Network (CNN) delivered the highest raw classification performance. When trained on the full, preprocessed dataset the CNN reached the top accuracy (99.59%), with very few misclassifications, showing outstanding precision and recall on both monocrystalline and polycrystalline subsets. This result confirms that an end-to-end deep model is highly effective at learning the spatial patterns in EL imagery, albeit at a very high computational cost.

The Wavelet Scattering Transform used with a committee of classical classifiers produced the best trade-off between accuracy and computational efficiency. The scattering-based pipeline achieved 98.56% overall accuracy on the preprocessed expanded dataset and produced near-perfect class reports in the per-subset tables, demonstrating that mathematically defined, multiscale features can reliably replace learned filters while keeping runtime and memory requirements low. This makes the method particularly attractive for embedded or low-power inspection systems.

The hybrid approach, Wavelet Scattering feeding a lightweight neural network, achieved slightly lower but still robust performance, around 98% depending on the configuration. The transfer-learning model based on a fine-tuned VGG16 produced competitive but lower accuracy than the other and exhibited a high computational cost among the tested architectures. The VGG16 variant showed more misclassifications in the test runs (higher counts of false positives / false negatives) and, given its processing and memory demands, it was found to be less attractive for embedded or constrained-hardware deployment despite acceptable classification performance.

Taken together, the comparative analysis indicates a clear trade-off: the CNN attains the highest absolute accuracy but requires the most computational resources, while the Wavelet Scattering + classical classifier pipeline attains elevated accuracy with a significantly lower computational cost, making it the most practical choice when processing resources or energy budget are constrained. The hybrid WST+DL and the VGG16 fine-tuned model occupy intermediate positions in this trade space. These conclusions are summarized in Table 1, which balances accuracy and computational cost in selecting the most suitable approach for different deployment scenarios.

Table 1: Comparison between the models results.

Model	Accuracy (%)			
	Larger Dataset		Reduced Dataset	
	Original Images	Preprocessed Images	Original Images	Preprocessed Images
CNN	73.51	99.59	83.33	100.00
WST + Classical Classifiers	75.97	98.56	89.16	100.00
WST + Neural Network	78.44	97.95	88.33	98.33
Transfer Learning (VGG16)	83.57	96.71	94.17	100.00

6. Conclusion

This study demonstrated the feasibility and effectiveness of using machine learning to automate defect detection in photovoltaic (PV) modules based on electroluminescence (EL) imaging. By comparing different architectures and training configurations, it was shown that preprocessing significantly enhances classification performance and generalization.

Among the evaluated approaches, all models achieved high accuracy on the preprocessed expanded dataset. The Convolutional Neural Network (CNN) reached the highest accuracy (99.6%), confirming the strong potential of deep learning for feature extraction, though at high computational cost. On the other hand, the Wavelet Scattering Transform (WST) combined with classical classifiers achieved nearly comparable accuracy (98.6%) but with substantially lower complexity, representing the most balanced and practical solution for embedded and large-scale inspection systems.

Future research should focus on expanding and diversifying the dataset to further improve model robustness under varying image conditions. Enhancing the preprocessing pipeline, particularly through geometric correction and automated cell segmentation, could also increase the number and quality of training samples. Moreover, optimizing computational efficiency through hyperparameter tuning and lightweight architectures would facilitate real-time deployment in embedded or low-power environments.

7. Acknowledgments

The authors would like to express their sincere gratitude to the Federal Fluminense University (UFF) for the institutional support provided throughout this research. The computational infrastructure and experimental resources made available by the Photovoltaic Applications Laboratory (LAF-UFF) were essential for the successful completion of this study. Research work carried out within the scope of the activities of the National Institute for Technological Development of Photovoltaic Solar Energy Applications, INCT-DAESF, CNPq/MCTI/Brazil, Process 408486/2024-4, FAPESP Process 2025/26902-8 and CAPES.

8. References

A. Alvim, G. Figueiredo. A importância da eletroluminescência no controle de qualidade das instalações fotovoltaicas. *SBSE 2023: Simpósio Brasileiro de Sistemas Elétricos*.

A. Mellit, S. Kalogirou, 2021. Artificial intelligence and internet of things to improve efficacy of diagnosis and remote sensing of solar photovoltaic systems: Challenges, recommendations and future directions. Renewable and Sustainable Energy Reviews, vol. 143. DOI: 10.1016/j.rser.2021.110889.

C. Buerhop-Lutz *et al.*, 2018. A Benchmark for Visual Identification of Defective Solar Cells in Electroluminescence Imagery. *35th European Photovoltaic Solar Energy Conference and Exhibition, 1287-1289*. DOI:

10.4229/35THEUPVSEC20182018-5CV.3.15.

G. Figueiredo, Marcelo Pinho Almeida, Alex Manito, e Roberto Zilles, 2018. Alternativa de baixo custo para imagens em eletroluminescência de módulos fotovoltaicos. *Congresso Brasileiro de Energia Solar*. DOI: 10.59627/cbens.2018.321

I. De La Parra, M. Muñoz, E. Lorenzo, M. García, J. Marcos, e F. Martínez-Moreno, 2017. PV performance modelling: A review in the light of quality assurance for large PV plants, Renewable and Sustainable Energy Reviews, vol. 78, p. 780–797. DOI:10.1016/j.rser.2017.04.080.

IEC Technical Specification 60904-13. Photovoltaic devices – Part 13: Electroluminescence of photovoltaic modules, 2018.

IEC Technical Specification 61215-1. Terrestrial photovoltaic (PV) modules - Design qualification and type approval - Part 1: Test requirements, 2021.

M. Dhimish, 2021. Defining the best-fit machine learning classifier to early diagnose photovoltaic solar cells hot-spots. Case Studies in Thermal Engineering, vol. 25. DOI: 10.1016/j.csite.2021.100980.

M. Köntges, M. Siebert, D. Hinken, U. Eitner, K. Bothe, e T. Potthof, 2009. Quantitative Analysis of PV-Modules by Electroluminescence Images for Quality Control. *24th European Photovoltaic Solar Energy Conference*, vol. 21-25. DOI: 10.4229/24THEUPVSEC2009-4CO.2.3.

M. Y. Demirci, N. Beşli, e A. Gümüşçü, 2021. Efficient deep feature extraction and classification for identifying defective photovoltaic module cells in Electroluminescence images. Expert Systems with Applications, vol. 175. DOI: 10.1016/j.eswa.2021.114810.

M. W. Akram *et al.*, 2018. CNN based automatic detection of photovoltaic cell defects in electroluminescence images. Energy, vol. 189. DOI: 10.1016/j.energy.2019.116319.

R. Ebner, B. Kubicek, e G. Ujvari. Non-destructive techniques for quality control of PV modules: Infrared thermography, electro- and photoluminescence imaging. *IECON 2013: 39th Annual Conference of the IEEE Industrial Electronics Society*, Vienna, nov. 2013, p. 8104–8109. DOI: 10.1109/IECON.2013.6700488.

S. Deitsch *et al.*, 2021. Segmentation of photovoltaic module cells in uncalibrated electroluminescence images. Machine Vision and Applications, vol. 32, no 4, p. 84. DOI: 10.1007/s00138-021-01191-9.

S. Deitsch *et al.*, 2019. Automatic classification of defective photovoltaic module cells in electroluminescence images. Solar Energy, vol. 185, p. 455–468. DOI: 10.1016/j.solener.2019.02.067.

T. Fuyuki, H. Kondo, Y. Kaji, A. Ogane, e Y. Takahashi, 2007. Analytic findings in the electroluminescence characterization of crystalline silicon solar cells. Journal of Applied Physics, vol. 101, no 2. DOI: 10.1063/1.2431075.

T. Fuyuki, H. Kondo, T. Yamazaki, Y. Takahashi, e Y. Uraoka,2005. Photographic surveying of minority carrier diffusion length in polycrystalline silicon solar cells by electroluminescence. Applied Physics Letters, vol. 86, no 26. DOI: 10.1063/1.1978979.

T. Mchedlidze, A. Herguth, e J. Weber, 2016. Monitoring of Si-solar cell degradation with electroluminescence, Solar Energy Materials and Solar Cells, vol. 155, p. 38–42. DOI: 10.1016/j.solmat.2016.05.008.

U. Jahn, M. Herz, M. Köntges, D. Parlevliet, M. Paggi, e I. Tsanakas, 2018. Review on infrared and electroluminescence imaging for PV field applications: International Energy Agency Photovoltaic Power Systems Programme: IEA PVPS Task 13, Subtask 3.3: report IEAPVPS T13-12:2018. Paris: International Energy Agency.

Y. Wang *et al.*, 2021. Adaptive automatic solar cell defect detection and classification based on absolute electroluminescence imaging. Energy, vol. 229. DOI: 10.1016/j.energy.2021.120606.

W. Tang, Q. Yang, K. Xiong, e W. Yan, 2020. Deep learning based automatic defect identification of photovoltaic module using electroluminescence images. Solar Energy, vol. 201, p. 453–460. DOI: 10.1016/j.solener.2020.03.049.